MODELLING SPACE DEBRIS ORBITS BY SYMPLECTIC MAPPING TECHNIQUE

Sławomir Breiter
Astronomical Observatory of the A. Mickiewicz University, Słoneczna 36, PL 60-286 Poznań, Poland.
E-MAIL: breiter@phys.amu.edu.pl

Gilles Métris
Observatoire de la Côte d'Azur/CERGA, Av. Copernic, F 06-130Grasse, France.
E-MAIL: metris@obs-azur.fr

ABSTRACT

We present the preliminary results of modelling the long-term dynamical evolution of space debris by means of a symplectic mapping technique. The mapping we use is an implicit, first-order integrator applied to averaged equations of motion, with a step equal to the orbital period. The method guarantees the absence of spurious secular trends in semi-major axis, eccentricity and inclination. In its preliminary version, our integrator includes zonal harmonics up to degree 4, resonant tesseral harmonics up to degree and order 6, Lunar and Solar perturbations, direct Solar radiation pressure, and atmospheric drag. We demonstrate the application of our software in the problems of GTO objects lifetime and LEO objects breakup.

1. INTRODUCTION

Like other orbital problems of celestial mechanics, the problem of space debris may require accurate integrators for particular objects and faster, but less accurate, algorithms to obtain some qualitative information about a great number of objects. The latter class usually contains analytical and semi-analytical theories. The method presented in this paper is semi-analytical, which means that we numerically integrate analytically averaged equations of motion. The salient feature of our theory is the use of a low order symplectic integrator – namely, the implicit, generating function, order one integrator[1]. When combined with the particular integration step like an unperturbed orbital period or a period of a perturbing force, such integrator is usually called a symplectic mapping.

2. THE METHOD AND SOFTWARE

In this paper we describe the version of our method as implemented in the FORTRAN package dubbed "SYMPSAT 1". When discussing the perturbing forces, we only focus on some non-typical details introduced during the development of the program.

2.1 Integrator

The process of integrating the motion consists of reapeted integrator steps – each jumping over the interval of one orbital period τ (the value of τ contains first-order contribution of J_2 harmonic). One can also interpolate between the endpoints of two steps taking some fraction of τ. We follow the trajectory of an object in Poincaré variables x_i, X_i related to the classical Dealaunay set as

$$\begin{aligned} x_1 &= l+g+h, \\ X_1 &= L, \\ x_2 &= -\sqrt{2(L-G)}\,\sin(g+h), \\ X_2 &= \sqrt{2(L-G)}\,\cos(g+h), \\ x_3 &= -\sqrt{2(G-H)}\,\sin h, \\ X_3 &= \sqrt{2(G-H)}\,\cos h, \end{aligned} \tag{1}$$

with uppercase momenta and lowercase coordinates. At the n-th step of integration we solve by iterations (on average 4 iterations per step) a set of implicit equations

$$\begin{aligned} X_i^{(n)} &= X_i^{(n-1)} + \tau\, F_i(X^{(n)}, x^{(n-1)}, t^{(n-1)}), \\ x_i^{(n)} &= x_i^{(n-1)} + \tau\, f_i(X^{(n)}, x^{(n-1)}, t^{(n-1)}), \\ t^{(n)} &= t^{(n-1)} + \tau. \end{aligned} \tag{2}$$

The right-hand sides F_i, f_i are the sums of Hamiltonian and dissipative (only atmospheric drag in our case) contributions

$$\begin{aligned} F_i &= -\frac{\partial \langle K \rangle}{\partial x_i} + \left\langle \dot{X}_i^{[\mathrm{drag}]} \right\rangle, \\ f_i &= \frac{\partial \langle K \rangle}{\partial X_i} + \left\langle \dot{x}_i^{[\mathrm{drag}]} \right\rangle. \end{aligned} \tag{3}$$

K is the Hamiltonian function of the problem and the time derivatives labelled "[drag]" are derived from

Gauss equations. The symbol $\langle\ \rangle$ denotes the average with respect to the mean anomaly, evaluated along a Keplerian orbit. In the absence of dissipative forces, the mapping defined by Eq. 2 has no spurious secular trends in energy and action-like variables; the secular error in angles is only linear in time[1]. After including a weak drag perturbing the motion, we still have a mapping with remarkable stability properties[2].

One special property of the mapping considered is worth noting: although we integrate a mean trajectory, the echo of a short-periodic noise re-enters the output as a numerical artifact inherent to all symplectic integrators. The amplitude of these numerically generated oscillations depends on the order of the integrator and on the time-step. Our practice shows, that with the first-order mapping and with τ equal to one orbital period, we obtain an amplitude comparable to that of short-periodic perturbations, although it is not a strict rule.

2.2 Hamiltonian perturbations

Being interested in qualitative effects only, we averaged all the perturbing potentials only at the first order. The important exception is the potential of J_2 harmonic – the libration of the argument of perigee can occur only at the second order of the averaging transformation. For the terms in J_2^2 we take the "centered" Hamiltonian of Métris and Exertier[3]. Wherever possible, we do not introduce the expansions in powers of eccentricity, thus aiming at the application of the "SYMPSAT" for high-eccentricity orbits. This requirement is satisfied in all zonal terms of the geopotential (we take J_2, J_3, and J_4 harmonics), in a lunisolar potential and in a direct radiation pressure potential.

The lunisolar potential depends on the positions of the Sun and the Moon; simple (but not Keplerian!) ephemerides for the perturbing bodies are based on the formulas given in *The Astronomical Almanac*[4] on pages C24 and D46. As an option, one can use doubly averaged potentials independent of the longitudes of the Moon or the Sun. For the Moon, as well as for the Sun, we take only the term with the second degree Legendre polynomial P_2 from the classical expansion of the perturbing function.

In the direct radiation pressure potential we adopt a traditional simplification neglecting the difference between the vectors Earth–Sun and satellite–Sun. We also assume a constant value for the factor

$$(\text{reflectivity coefficient}) \times \frac{\text{satellite surface}}{\text{satellite mass}}.$$

Tesseral harmonics of the geopotential may produce significant long-periodic effects only when a resonance occurs. In this part, having not found another way, we adopted the expansion of Kaula–Wnuk[5] in powers of eccentricity. The harmonics up to degree and order 6 are included, and the allowed maximum power of the eccentricity is limited only by practical factors like computer memory available and computation time. At the beginning of the integration, all possible frequencies are checked, and resonant combinations of indices are stored. The eccentricity functions of Kaula $G(e)$ and their derivatives $G'(e)$ required for the resonant terms are tabulated at 8 values of e; father in the program this grid serves to evaluate cubic splines or – for some functions – a "quasi-quadratic" approximation. The latter is

$$G_{l,p,q}(e) \approx e^{|q|}\ \left(A + B\,e^2\right), \qquad (4)$$

very efficient for $e < 0.1$ when applied to all eccentricity functions except $G_{l,p,0}(e)$, and to all derivatives except $G'_{l,p,\pm1}(e)$; it requires only two constants A, B to be stored. The combination of these two methods guarantees the relative error of $G(e)$ or $G'(e)$ not exceeding 10^{-4} for $e < 0.1$, or 10^{-2} for $e < 0.9$.

2.3 Drag perturbations

Averaging the influence of atmospheric drag is difficult for two well known reasons: 1.) it is hard to give an accurate model for the physical state of the atmosphere, 2.) the quadratures occuring in Gauss equations are too complicated for analytical expressions. "SYMPSAT" permits any atmosphere density model to be included, but in the first version we take only the model of Jacchia et al. for $T_\infty = 1000\,\mathrm{K}$, as given in Ref. 6. We derived polynomial approximations for the logarithm of density as functions of the inverse of altitude

$$\log(\rho) \approx \sum_{k=0}^{6} a_k\,(1/h)^k, \qquad (5)$$

with four sets of a_k coefficients for different intervals of $1/h$. The relative error of density computed from this approximation is less than 0.006. We added a quadratic extrapolation beyond $h = 2500$ km

$$\begin{aligned}\log(\rho) \quad \approx \quad & -40.28608 + 1.125714/h \\ & +0.0367/h^2, \end{aligned} \qquad (6)$$

where h should be expressed in Earth radii, and ρ is in $\mathrm{kg/m^3}$.

The perturbing force depends on the velocity of a satellite with respect to the atmosphere. We assumed that the atmosphere has the angular velocity of Earth rotation, and in all expressions we neglected

the squares of the ratio

$$\frac{\text{Earth rotation rate}}{\text{satellite mean motion}}.$$

We can state, that our assumptions are to a large extent compatible with those of Sterne[7]. For the purpose of "SYMPSAT" we derived Gauss equations for drag effects in Delaunay variables from the scratch – they are given in a special report available from the first author upon request.

Averaging required the evaluation of quadratures of a general type

$$Q = \int_{-\pi}^{\pi} \rho(\vartheta)\, W(\vartheta)\, d\vartheta. \qquad (7)$$

where ϑ is the true anomaly (actually, wherever it is more convenient we switch to eccentric anomaly instead). The presence of density ρ as a factor implies a rapid drop of the value of ρW away from the perigee $\vartheta = 0$, even for moderate eccentricities. On the other hand, when e is small, the integrand ρW is either almost sinusoidal or almost constant. To evaluate Q we start by checking the ratio

$$\alpha = \left| \frac{\rho(0)\, W(0)}{\rho(\pi)\, W(\pi)} \right|. \qquad (8)$$

When α is less than some treshold value (usually between 50 and 300) we can approximate the integral Q by a three-point ($\vartheta = 0, \pi/2, \pi$) trapezoid rule. Otherwise, we take the approximation of Zeldovich and Myškis[8]

$$Q \approx \rho(0)\, W(0) \sqrt{2\pi \left| \frac{\rho(0)\, W(0)}{[\rho(0)\, W(0)]''} \right|}. \qquad (9)$$

The relative error of so computed Q does not exceed 0.15 in most cases and it tends to zero when the eccentricity diminishes. This approximation works really fast, and the error of 0.15 is acceptable taking into account all simplifications concerning the state of atmosphere.

3. EXEMPLARY APPLICATIONS

Our "SYMPSAT 1" is a basic version, still requiring further development, but it can already be exploited in quite various problems concerning the orbital motion. In all the examples we give, the ratio of the effective surface to the mass 0.01 m^2/kg was taken (the same for a satellite or its fragment) and the reflectivity coefficient was 1.14. The programs were executed on a PC 486DX2 and on a SUN SPARC 20 (2×125 MHz).

3.1 Low orbits

As a first example we trace the orbital evolution of a swarm of 1000 of fragments originating from a parent satellite. The satellite's orbit had the apogee altitude $h_q = 648$km, $e = 0.00815$, $i = 90°.01$, $\omega = 70°$, and $\Omega = 80°$. We assumed an isotropic explosion adding 750 m/s to each fragment, and the orientation of this velocity increment was randomly generated. The results are presented in Fig. 1. Only 545 pieces survived the first 90 minutes and then their spatial distribution became more and more isotropic, with 447 pieces remaining after 4 years.

3.2 Geosynchronous transfer orbits

The second application was inspired by the work of Siebold and Reynolds[9], discussing the dependence of a GTO lifetime on the initial orientation of the orbit with respect to the Sun. Figure 2 (compare with Fig. 5 in Ref. 9) shows the results obtained for a given perigee altitude of 250 km and apogee altitude of 35758 km, the argument of perigee being $\omega = 0$. We show the dependence of the lifetime on the right ascension of the Sun α and on the right ascension of the satellite's ascending node Ω (thus on the day and hour of launch respectively) for different values of orbital inclination i. Our model of orbital motion is more elaborated than in Ref. 9 (we take more perturbing factors into account). The semi-analytical character of our mapping allows to avoid the problems at certain values of inclination where the analytical formulas of Siebold and Reynolds[9] break down; we note especially $i \approx 46.°37$, where the denominator $\dot{\omega} + \dot{\Omega}$ tends to zero. We must acknowledge however, that the purely analytical approach of Ref. 9 is probably more efficient for orbits permitting its application. The problem is indeed fairly time-consuming for "SYMPSAT", if one requires a dense grid of α and Ω. We took a grid of 100×100 points and each ficticious satellite was integrated on the interval of 30 years (unless it re-entered the atmosphere before reaching this age). A test run – practically equivalent to integrating more than 10^8 revolutions of a single satellite – took about 4000 minutes on SPARC.

4. ACKNOWLEDGEMENTS

The work presented in this paper was financed by the Polish Committee of Research (KBN) grant 2 PO3C 006 08. The travels of the authors to Grasse and Poznań were sponsored by the French Ministry of Foreign Affairs and by KBN.

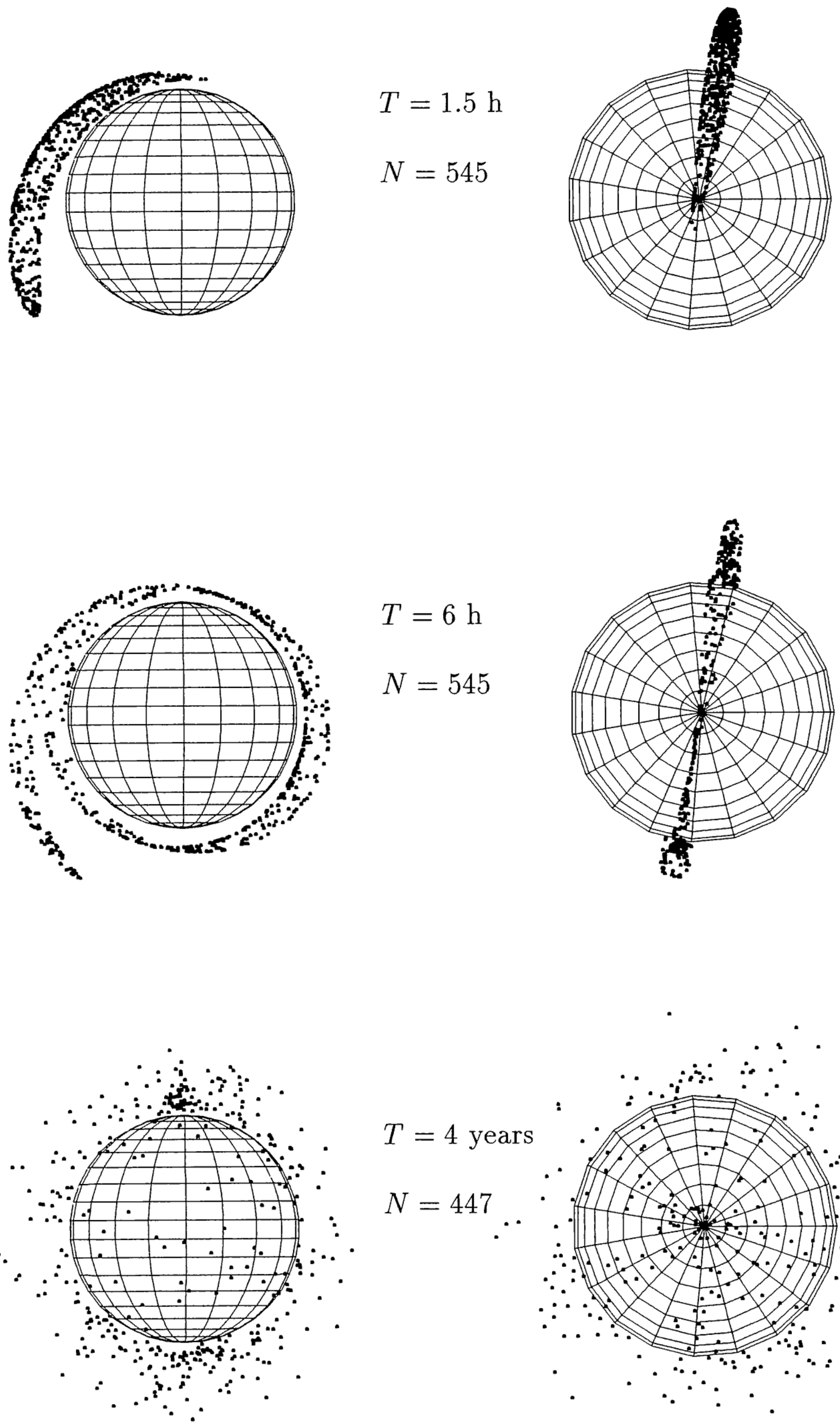

Figure 1. The evolution of a swarm of fragments resulting from a ficticious explosion of a low satellite (see Sect. 3.1). To the left, the view from a direction perpendicular to the initial orbital plane of a the primary object; to the right – from above the North Pole. N is the number of fragments, T is the time after the esplosion

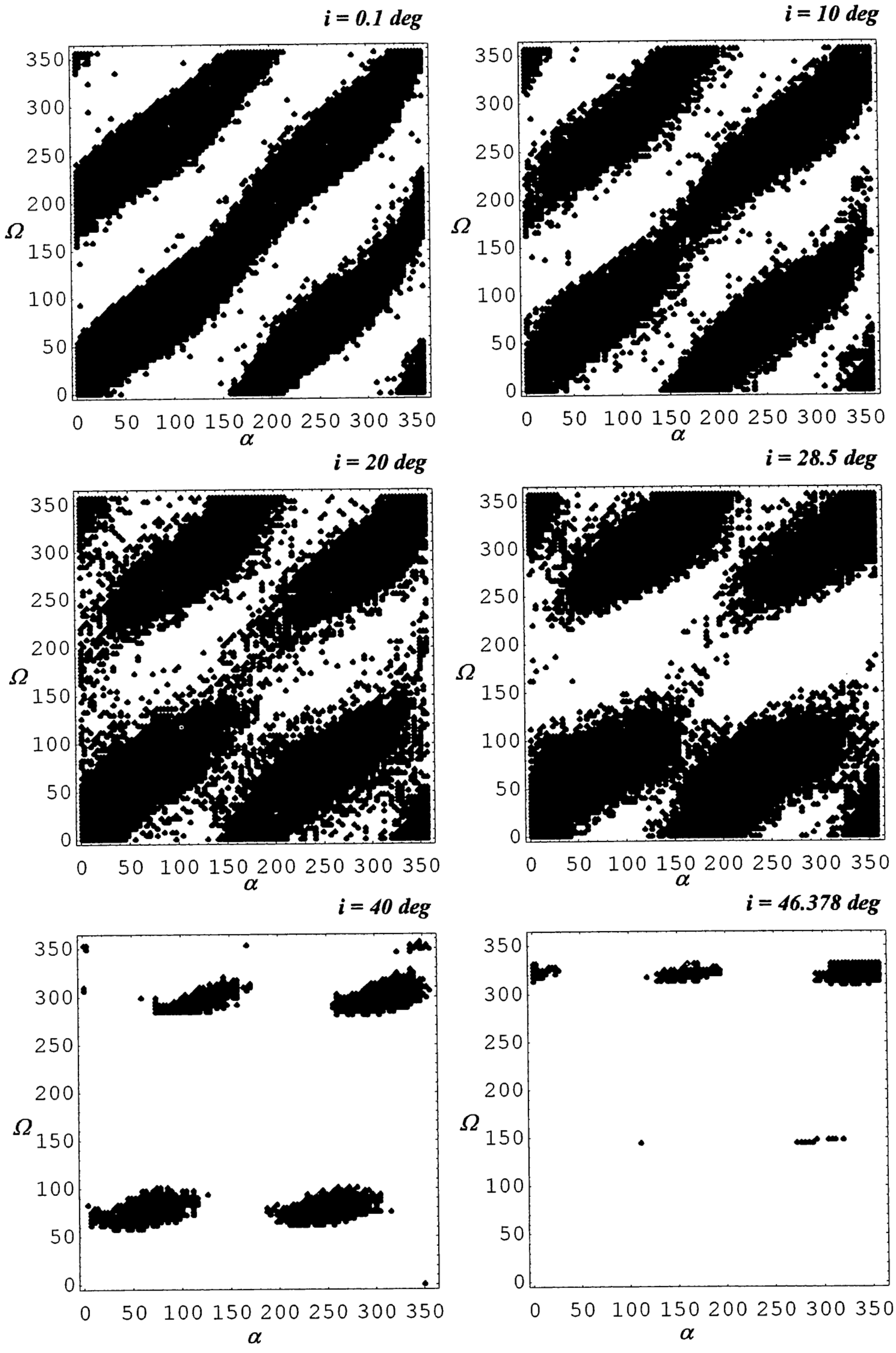

Figure 2. Long life orbits for GTO objects with an initial perigee altitude 250 km (see Sect. 3.2). Black dots mark these couples of initial right ascensions of the Sun α and of the ascending node Ω, for which an object remains in space at least for 20 years. Each plot was obtained for a different initial inclination i.

5. REFERENCES

1. Yoshida, H., Recent Progress in the Theory and Application of Symplectic Integrators, *Celestial Mechanics and Dynamical Astronomy*, Vol. 56, 27-53, 1993.
2. Zhou, J., et al., Mapping Models for Near-Conservative Systems with Applications, *Celestial Mechanics and Dynamical Astronomy*, Vol. 60, 471-487, 1994.
3. Métris, G. and Exertier, P., Semi-Analytical Theory of the Mean Orbital Motion, *Astronomy and Astrophysics*, Vol. 294, 278-286, 1995.
4. The Astronomical Almanac for the Year 1993, Washington/London, 1992.
5. Wnuk, E., Tesseral Harmonic Perturbations for High Order and Degree Harmonics, *Celestial Mechanics*, Vol. 44, 179-192, 1989.
6. Zarrouati, O., *Trajectoires Spatiales*, CEPADUES, Toulouse, 129-130, 1987.
7. Sterne, T., E., Effect of the Rotation of a Planetary Atmosphere upon the Orbit of a Close Satellite, *American Rocket Society Journal*, Vol. 29, 777-782, 1959.
8. Zeldovich, Ya., B. and Myškis, A., D., *Elements of Applied Mathematics*, Mir, Moscow, 76-82, 1976.
9. Siebold, K. H. and Reynolds, R., C., Lifetime Reduction of a Geosynchronous Transfer Orbit with the Help of Lunar-Solar Perturbations, *Advances in Space Research*, Vol. 16, No. 11, (11)155-(11)161, 1995.